Dynamic Friedel oscillations on the surface of a topological insulator

V. A. Stephanovich,[1,*] E. V. Kirichenko,[1] V. K. Dugaev,[2,†] and J. Barnaś[3,4]
[1]*Institute of Physics, Opole University, 45-052 Opole, Poland*
[2]*Department of Physics and Medical Engineering, Rzeszów University of Technology, aleja Powstańców Warszawy 6, 35-959 Rzeszów, Poland*
[3]*Faculty of Physics, Adam Mickiewicz University, ulica Umultowska 85, 61-614 Poznań, Poland*
[4]*Institute of Molecular Physics, Polish Academy of Sciences, ulica M. Smoluchowskiego 17, 60-179 Poznań, Poland*

(Received 21 August 2021; revised 8 January 2022; accepted 6 February 2022; published 14 February 2022)

We study theoretically the dynamic Friedel oscillations of electrons at the surface of a topological insulator (TI) that are generated by the rotation of a localized impurity spin. We show that the spin-orbit interaction (SOI) in Rashba form, which is an integral part of the TI Hamiltonian, yields a highly anisotropic response to the localized spin rotation. As a result, the response to a flip of a localized spin z projection involves the reaction of all x, y, and z components of the local magnetization. Additionally, the dynamic spin moment (and thus also Friedel oscillations) emitted by the localized dynamical spin depends on the orientation in the TI plane. The resulting unusual dynamics is due to the interplay of SOI and Ruderman-Kittel-Kasuya-Yoshida interactions. This provides the basis for manipulation of the spin transport in topological insulators decorated with localized impurity spins, which may be important for technological applications.

DOI: 10.1103/PhysRevB.105.075306

I. INTRODUCTION

The notion of Friedel oscillations appears in the quantum mechanical description of localized charge screening in the gas or liquid of mobile carriers [1]. It is well known that such oscillations occur near localized defects in metallic or semiconducting materials [2]. However, they can also occur in other conducting materials, like in currently investigated topological insulators (TIs). These materials have unique transport properties—they are insulating (semiconducting) in the bulk and conducting at the surfaces due to topologically protected gapless (metallic) surface states [3]. A characteristic property of these states is the so-called spin-momentum locking. In other words, the orientation of the electron spin in the surface topological states is locked by spin-orbit interaction (SOI) in the state perpendicular to the corresponding electron momentum [4–10]. This makes TIs promising materials for low-dissipation spintronic applications [6,7]. Interestingly, SOI also plays an important role in the ultrafast (subpicosecond) dynamics and relaxation of impurity spins localized at the TI surface (see Ref. [10] and references therein). If the spins of localized impurities rotate, the relevant spin correlations occur *via* the indirect exchange interaction, which is mediated by the dynamic Friedel oscillations of the TI surface electron density [11–13]. The latter interaction, known as Ruderman-Kittel-Kasuya-Yoshida (RKKY) [1], plays a significant role in the spin-spin response of TIs [14,15].

In this paper, we consider the dynamical response of surface electrons to the dynamics of the magnetic impurity or surface imperfection (like a defect [16], step edge, or adsorbate [17]) with large (classical) spin at the surface of a topological insulator. The above defects can be placed at the TI surface, for instance, by a spin-polarized scanning tunneling microscope (STM). The problem of static response was already discussed in several papers [14,15,18–20]. Here, we analyze the dynamics of magnetic response to a fast flip of the above classical impurity spin. The motivation of our analysis is that with the appearance of fast (in the picosecond range) time-dependent electron transfer techniques [21,22] and laser-induced subpicosecond magnetic switching [23], the question arises of how the above phenomena influence the time-dependent response of the electron gas on the TI surface. Furthermore, in the presence of spin-orbit coupling and hence spin-momentum locking in a TI, it is clear that the transient electric current should somehow depend on the spin response of the electron gas on the TI surface. Such a time-dependent response is known to be an important ingredient in spintronic and terahertz-emitting devices [24]. It is thus of interest to study theoretically the time-resolved RKKY mechanism in topological insulators.

The simplest description of the collective spin dynamics is based on the phenomenological approach of Landau and Lifshitz [25], in which the spin response obeys the Landau-Lifshitz-Gilbert (LLG) equation (see Ref. [23] for references). To describe theoretically magnetic relaxation and fast spin switching in two-dimensional (2D) systems, both the above-mentioned LLG approach and microscopic quantum mechanical calculations [13,26–28] can be utilized in general. The quantum mechanical model is usually formulated in terms of the dynamic RKKY [1] interaction and is used primarily when the localized spin rotation occurs on a femtosecond timescale. In turn, the LLG collective dynamics, being driven by correlated spin clusters of macroscopic dimensions,

*stef@uni.opole.pl
†vdugaev@prz.edu.pl

occurs on a much slower (picosecond) timescale [29,30]. *Ab initio* simulations of localized impurity spin dynamics in a semiconductor host were performed recently [31,32] within the RKKY-based quantum approach. The same approach has been applied to graphene, where, contrary to TIs, the SOI contribution is almost negligible [33–35].

It has been shown that Rashba SOI twists the ordinary RKKY interaction in one-dimensional and 2D systems [36]. However, the dynamic consequences of this twisting and its synergy with linear electron dispersion in TIs has not been considered yet. On the other hand, the dynamics of *pure* (i.e., without SOI) RKKY interaction was studied recently [37]. Following the recent publications [36,37], we consider here the dynamical Friedel oscillations in a 2D electron gas formed on the surface of a topological insulator and show that the twisting effects appear in the dynamical case as well. For instance, the tight coupling of spin and momentum in the surface topological states due to spin-momentum locking induces the ordinary electric (charge) current. As this current is induced by a rotating localized spin (rather than by electric charges flow as in an ordinary metal), it is dynamic in its nature and vanishes in the static case. Being proportional to the dynamic spin, it decays after a certain time proportional to the time of localized spin rotation. To be more specific, we study here the response of the 2D electron gas at the surface of TI to a fast reversal of a single impurity spin $\mathbf{S}_0(t)$ coupled to the electrons by direct exchange interaction. The magnetic polarization of the electron gas appears in the form of the time-dependent Friedel oscillations, which now not only become noticeably dependent on the SOI constant γ (proportional to the Fermi velocity v_F) but also become highly anisotropic. In other words, the flip of one component (say, S_z) of a localized spin in the topological surface states induces dynamic polarization of all three spin components. Accordingly, all nine components of the spin response tensor S_{ij} $(i, j = x, y, z)$, describing the response of the ith spin component to the flip of the jth one, become nonzero. Our results also reveal different ways of generating alternating electric currents in TIs by manipulating the SOI parameter.

In Sec. II we present the model Hamiltonian used in this paper and derive the corresponding Green's function in the time domain. The dynamic response to a single impurity spin reversal is derived in Sec. III, where the corresponding numerical results are also presented and discussed. A summary and outlook are given in Sec. IV.

II. MODEL

We consider surface electrons in a TI with SOI in the Rashba form. These 2D electrons are described by a Hamiltonian in the following matrix form:

$$\mathcal{H} = -\gamma\,(k_y\sigma_x - k_x\sigma_y) + \frac{g}{n}\,\boldsymbol{\sigma}\cdot\mathbf{S}_0(t), \tag{1}$$

where $\gamma = \hbar v_F$ is the SOI constant, v_F is the Fermi velocity, $n = N/A$ is the areal density of the host atoms (A is the area of the 2D electronic system, and N is the total number of host atoms), g is the local exchange coupling constant, $\boldsymbol{\sigma} = (\sigma_x, \sigma_y, \sigma_z)$ is a vector of Pauli matrices, and $\mathbf{S}_0(t)$ is the dynamic spin of a magnetic impurity.

The first term in the Hamiltonian (1) can be identically rendered to the form

$$\mathcal{H}_{\rm SOI} = \gamma\hat{\mathbf{z}}\cdot(\boldsymbol{\sigma}\times\mathbf{k}) \equiv \gamma\boldsymbol{\sigma}\cdot(\mathbf{k}\times\hat{\mathbf{z}}), \tag{2}$$

where $\hat{\mathbf{z}}$ is the unit vector along the z axis and we have used the cyclic property of a triple product. The structure of expression (2) shows that the spin of the electron having momentum $\hbar\mathbf{k}$ is oriented along the vector $\mathbf{k}\times\hat{\mathbf{z}}$, i.e., the electron spin orientation is "locked" to its momentum. This phenomenon is called *spin-momentum locking* (SML) and is inherent in the systems with SOI (see, e.g. [10]). Below we shall use this effect to calculate the electric current, which flows only in systems with SOI, which is related to the spin-momentum locking. Note that kinetic terms in the Hamiltonian like $\hbar^2k^2/(2m^*)$ (m^* is the carrier effective mass) "unlock" the spin and momentum, suppressing the latter current.

The exchange interaction between itinerant electrons on the TI surface and localized spin $\mathbf{S}_0(t)$ generates dynamic Friedel oscillations of the electron spin density around the localized spin $\mathbf{S}_0$. The relevant expression for the TI response to an impurity spin rotation can be obtained from the perturbation theory with respect to the coupling constant g [1]. Following the usual procedure, we first construct the unperturbed Green's function of the problem. The easiest way to do this is to invert the Hamiltonian (1). To be specific, the expression for the inverse Green's function reads [36]

$$G^{-1}(\varepsilon, \mathbf{k}) = \zeta\sigma_0 + \gamma(k_y\sigma_x - k_x\sigma_y), \quad \zeta = \varepsilon + i0, \tag{3}$$

where ε is the energy and σ_0 stands for the unit matrix. Inversion of the matrix in (3) yields

$$G(\varepsilon, \mathbf{k}) = \frac{\varepsilon}{\zeta^2 - \gamma^2k^2}\sigma_0 + \frac{\gamma(k_y\sigma_x - k_x\sigma_y)}{\zeta^2 - \gamma^2k^2}. \tag{4}$$

Expression (4) is suitable for the calculation of the above-mentioned spin response and other characteristics. However, as we are interested in the time domain properties, it is more convenient for our purpose to use the time representation of the Green's function (4). This is accomplished, as usual, by the expansion of the denominators in (4) into elementary fractions and integrating over the energy ε and wave vector $\mathbf{k}$ in the proper domains of $t - t'$. This procedure yields the following matrix structure of the Green's function in the time domain:

$$G_{>0}(\mathbf{r}, \mathbf{r}', t, t') = G^{(0)}_{>0}(\mathbf{r}, \mathbf{r}', t, t')\sigma_0 + i\hat{A}G^{(1)}_{>0}(\mathbf{r}, \mathbf{r}', t, t'), \quad t - t' > 0,\ k > k_F, \tag{5}$$

$$G_{<0}(\mathbf{r}, \mathbf{r}', t, t') = G^{(0)}_{<0}(\mathbf{r}, \mathbf{r}', t, t')\sigma_0 + i\hat{A}G^{(1)}_{<0}(\mathbf{r}, \mathbf{r}', t, t'), \quad t - t' < 0,\ k < k_F. \tag{6}$$

Here, the lower indices >0 and <0 stand for $t - t' > 0$ and $t - t' < 0$, respectively, $\hat{A} = \sigma_x\sin\alpha - \sigma_y\cos\alpha$, $\alpha = \arctan[(y - y')/(x - x')]$, and $k_F = E_F/\gamma$ is the Fermi momentum (accordingly, E_F is the Fermi energy). The angle α enters the problem *via* angular integration over $\mathbf{k}$ components. The origin of the angular dependence of the Green's function stems from the SOI structure in the initial Hamiltonian (1). This angular dependence is the source of all twists and anisotropies of the 2D indirect exchange interaction in the surface topological states. The anisotropy of the dynamic spin response, related to the dependence on the angle α, is

a characteristic feature of Friedel oscillations at the surfaces of TIs.

The explicit form of the Green's functions entering expressions (5) and (6) reads

$$G^{(0)}_{>0} = -i\frac{n}{4\pi}\int_{k_F}^{\infty} J_0(k|\mathbf{r}-\mathbf{r}'|)\, e^{-i(t-t')\varepsilon_-}\, kdk, \quad (7a)$$

$$G^{(1)}_{>0} = -i\frac{n}{4\pi}\int_{k_F}^{\infty} J_1(k|\mathbf{r}-\mathbf{r}'|)\, e^{-i(t-t')\varepsilon_-}\, kdk, \quad (7b)$$

$$G^{(0)}_{<0} = i\frac{n}{4\pi}\int_{0}^{k_F} J_0(k|\mathbf{r}-\mathbf{r}'|)\, e^{-i(t-t')\varepsilon_+}\, kdk, \quad (7c)$$

$$G^{(1)}_{<0} = i\frac{n}{4\pi}\int_{0}^{k_F} J_1(k|\mathbf{r}-\mathbf{r}'|)\, e^{-i(t-t')\varepsilon_+}\, kdk, \quad (7d)$$

$$\varepsilon_\pm = \frac{E_\mathbf{k}-E_F}{\hbar} \pm i\Gamma,$$

where $E_\mathbf{k} = \gamma k$ ($k = |\mathbf{k}|$) is the eigenvalue of the unperturbed Hamiltonian (1) and $J_{0,1}(z)$ are Bessel functions [38]. Here, $\Gamma = \hbar/2\tau$ is the electron momentum relaxation rate (τ is the corresponding relaxation time) related to the scattering of electrons by defects, impurities, etc. Below we shall use the Green's functions (5) and (6) to calculate the dynamic spin response.

III. DYNAMIC SPIN RESPONSE

Due to the SOI-induced anisotropic nature of surface electron states in TIs, the dynamic response function is determined by the spin response tensor S_{mn} ($m, n = x, y, z$), which describes the response of the mth electronic spin component to the rotation of the nth component of the impurity spin. This tensor actually reflects the twisting of spin density (and thus also of the Friedel oscillations) at the surface of the TI. The spatial and temporal dependence of the TI electronic spin response $\mathbf{R}(\mathbf{r}, t)$ on the rotation of a localized (impurity) spin $\mathbf{S}_0(t)$ in the lowest order of perturbation theory is given by the formula [25]

$$R_m(\mathbf{r}, t) = -\frac{ig}{\hbar}\sum_{n=x,y,z}\mathrm{Tr}\int_{-\infty}^{t} S_{mn}(\mathbf{r}, t, t')dt', \quad (8)$$

with

$$S_{mn}(\mathbf{r}, t, t') = \sigma_m G_0(\mathbf{r}, t, 0, t')\sigma_n S_{0n}(t')\, G_0(0, t', \mathbf{r}, t'), \quad (9)$$

where G_0 is the unperturbed Green's function taken in the appropriate domain $t - t' > 0$ (5) or $t - t' < 0$ (6), $m, n = x, y, z$, and Tr means a trace over the spin indices.

Having the expression for the spin response vector (8), we are in the position to derive the expression for the electric current, related to the above spin-momentum locking effect. The expression for the electric current operator can be obtained from the following general relation (see, e.g., [25]):

$$\hat{\mathbf{j}} = \frac{e}{\hbar}\frac{\partial\mathcal{H}}{\partial\mathbf{k}}, \quad (10)$$

where e is an electronic charge and $\mathcal{H}$ is the Hamiltonian (1) of our system. In the lowest order of perturbation theory with respect to the interaction constant g, the Hamiltonian $\mathcal{H}$ should be substituted for $\mathcal{H}_{\mathrm{SOI}}$ (2) so that the operatorial part of the expression for the electric current (10) reduces to

$$\hat{\mathbf{j}} = \frac{e\gamma}{\hbar}\hat{\mathbf{z}}\times\boldsymbol{\sigma}. \quad (11)$$

As the unit vector $\hat{\mathbf{z}}$ depends on neither time nor space, the averaging procedure (8) indicates that the observable value of the current $\mathbf{j}$ is proportional to the electronic spin response vector $\mathbf{R}(\mathbf{r}, t)$. Specifically,

$$\hat{\mathbf{j}} = \frac{e\gamma}{\hbar}\hat{\mathbf{z}}\times\mathbf{R}(\mathbf{r}, t), \quad (12)$$

where $\mathbf{R}(\mathbf{r}, t)$ is determined by expression (8). The possible experimental setup comprises a spin-polarized STM scanning tip placed on the TI surface. A latter tip is assumed to act effectively on the localized impurity spin with a magnetic field, directed perpendicular to the surface. This field tends to align the spin direction $\mathbf{S_0}$ of the above magnetic impurity with that of the tip. This activates a Larmor precession of $\mathbf{S_0}$ in the above magnetic field. The switching of STM magnetization along the z axis generates the rotation of the localized impurity spin in the xy plane, which is perpendicular to the z axis. To quantify the above character of impurity spin rotation, we consider the experimentally relevant case [37] when the y component of the spin has the form

$$S_{0y}(t) = \begin{cases} \tilde{S}_0\cos(\pi t/T), & |t| < T/2, \\ 0, & |t| \geqslant T/2, \end{cases} \quad (13)$$

where T is the spin-flip time. Substituting Eqs. (5) and (6) [also taking into account Eqs. (7a) to (7d)] into Eq. (8) and calculating the trace of Pauli matrices, we find that for the dynamic spin in the form (13), the electronic spin response consists of the components $R_x(\mathbf{r}, t)$ and $R_y(\mathbf{r}, t)$. This procedure gives identically $R_z \equiv 0$, which is consistent with the picture that the spin response occurs in only the TI plane. The explicit expressions for spin response components assume the form

$$R_x(\mathbf{r}, t) = -\frac{ig}{4\pi^2\hbar}\sin 2\alpha\int_{-\infty}^{t} S_{0y}(t')dt' \times\left\{\int_{k_F}^{\infty} e^{i\omega_{\mathbf{kk}_1}(t-t')}kdk\int_0^{k_F} J_1(kr)J_1(k_1r)k_1dk_1 - \int_{k_F}^{\infty} e^{i\omega_{\mathbf{kk}_1}(t-t')}k_1dk_1\int_0^{k_F} J_1(kr)J_1(k_1r)kdk\right\}, \quad (14)$$

$$R_y(\mathbf{r}, t) = -\frac{ig}{4\pi^2\hbar}\int_{-\infty}^{t} S_{0y}(t')dt'\left\{\int_{k_F}^{\infty} e^{i\omega_{\mathbf{kk}_1}(t-t')}kdk \times\int_0^{k_F} g_+(k, k_1, \alpha)k_1dk_1 - \int_{k_F}^{\infty} e^{i\omega_{\mathbf{kk}_1}(t-t')}k_1dk_1\int_0^{k_F} g_-(k, k_1, \alpha)kdk\right\}, \quad (15)$$

where

$$\omega_{\mathbf{k}\mathbf{k}_1} = \frac{E_{\mathbf{k}} - E_{\mathbf{k}_1} - 2i\Gamma}{\hbar},$$

$$g_{\pm}(k, k_1, \alpha) = J_0(kr)J_0(k_1 r) \pm \cos 2\alpha J_1(kr)J_1(k_1 r). \quad (16)$$

For the discussed experimental setup, which generates components $R_x(\mathbf{r}, t)$ and $R_y(\mathbf{r}, t)$ in the forms (15) and (16), the SML-related current components read

$$j_x(\mathbf{r}, t) = -\frac{e\gamma}{\hbar} R_y(\mathbf{r}, t), \quad j_y(\mathbf{r}, t) = \frac{e\gamma}{\hbar} R_x(\mathbf{r}, t). \quad (17)$$

This means that the electric current and the system spin response are "linked" to each other so that the properties of the SML-related current reduce to those of the spin response vector, although in the "rotor" form (12) and (17).

We see that the components of the spin response and current depend differently on the angle α. Really, while $R_x(\mathbf{r}, t)$ is proportional to $\sin 2\alpha$ and does not contain the angle α inside the integral, the component $R_y(\mathbf{r}, t)$ contains $\cos 2\alpha$ inside the integral, so that at $\alpha = 0$ (no SOI twisting of the exchange interaction) it gives the nonzero answer. This implies that for the case of an ordinary semiconductor with parabolic electronic dispersion, the dynamic localized spin $S_{0y}(t)$ (13) excites only the y component of the electronic gas spin response. Note also that in the latter case, there would be no SML effect, so that the electric current in the form (12) is substituted by the spin current. This result coincides with our previous consideration [37]. Moreover, while the R_y component is nonzero at any angle α (including $\alpha = 0$; see above), the R_x component is zero at $\alpha = 0$ and $\alpha = \pi/2$, achieving the maximal value at $\alpha = \pi/4$. This fact will be seen below in the numerical calculations.

Our analysis shows that the presented dependences (14) and (15) are the "building blocks" of any more sophisticated dependence of the spin response provided more complex rotations of impurity spin. For instance, the above rotation of the localized spin in the xy plane can admit the nonzero $S_{\alpha x}$ component. In this case, the response will also comprise the R_x and R_y components, each of which is a linear combination of the contributions (14) and (15). Note that for any other STM scanning patterns, any component of the spin response tensor S_{mn} can be easily calculated by taking traces of different combinations of the Pauli matrices in Eq. (9). These components will be essentially the same as those in Eqs. (14) and (15).

To present numerical results for the spin response vector components (14) and (15), we introduce normalized response functions $R_{x,y}/R_0$ and the following dimensionless variables: $R_0 = gk_F^4 \tilde{S}_0/(4\pi^2 E_F n^2)$, $x = E_F(t - t')/\hbar$, $y = k/k_F$, $y_1 = k'/k_F$, $t_0 = E_F t/\hbar$, $\tau_0 = E_F \tau/\hbar$, and $T_0 = E_F T/\hbar$. Figures 1(a)–1(c) show the spatial behavior of the spin response component R_y for $\alpha = 0$ and different values of t_0 and T_0, as indicated. We have chosen $\alpha = 0$, as the corresponding curves are then more distinguishable on the scale of the plots. Moreover, as we can note in Fig. 1(d), where the dependence on α is shown, the case $\alpha = 0$ corresponds to the most pronounced oscillations in the $R_y(z)$ dependence. We can see from Figs. 1(a)–1(c) that for small time, $t_0 = 1$, the electron spin polarization does not spread far from the source [i.e., from the magnetic impurity with spin rotating according

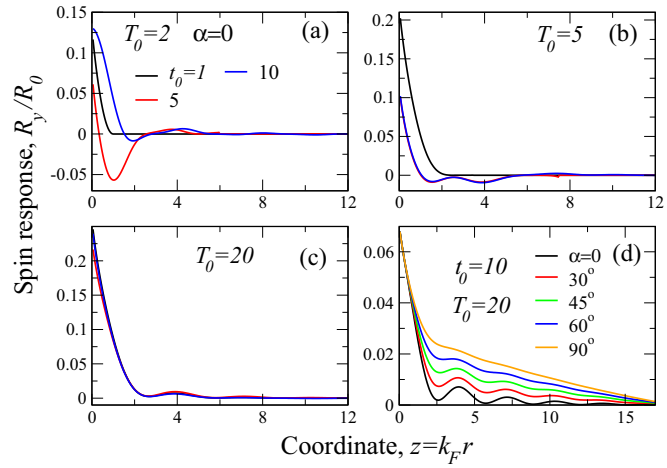

FIG. 1. Spin response component R_y oscillations for different dimensionless times t_0 [as explained in the legend in (a)]. (a)–(c) correspond to different T_0 as shown in each panel. (d) The α dependence of the parameters reported in the panel. For all panels $\tau_0 = 100$; in (a)–(c) $\alpha = 0$, as indicated in (a).

to Eq. (13)] on the TI surface. For instance, in Fig. 1(a) the response at $t_0 = 1$ spreads approximately up to $z = 1$ and then decays to zero. For $t_0 = 10$, the first pulse of the system response decays around $z_0 = 3$, and then it oscillates up to large values of z. At longer spin-flip times $T_0 = 5$ and 20, the curves for all t_0 (for $T_0 = 5$ this concerns only $t_0 = 5$ and 10) become indistinguishable because for $t_0 < T_0$ [which is the case for Fig. 1(c)] the system simply does not have enough time to respond for the impurity spin flip. This behavior is due to the synergy of SOI and the retardation of the TI surface response to the impurity spin flip, Eq. (13), which spoils the regular Friedel oscillations.

Figure 1(d) shows the angular dependence of R_y for typical experimentally relevant values $t_0 = 10$ and $T_0 = 20$. We have chosen the angular range $0^\circ < \alpha < 90^\circ$ due to the angular dependence in Eq. (16). To be specific, this angular dependence is defined by the factor $\cos(2\alpha)$, which is π periodic. Thus, the range $0^\circ < \alpha < 90^\circ$ (half period) covers all physically relevant cases. The choice of other parameters was dictated by the experimental situation in femtosecond optical switching: 12 fs [39] and 80 fs [30]. In turn, the electron momentum relaxation time is in the picosecond range, so that everywhere we assumed $\tau_0 = 100$. We can note that at large distances from the localized spin, $z = k_F r > 15$, the anisotropy vanishes, and the curves for different α merge into a single one. This shows that at large z the main characteristic features of TI due to SOI disappear. A similar effect was obtained in a recent work [40], where SOI was the underlying mechanism of chaotization of the internal motion in an exciton of finite radius.

The spatial dependence of the R_x component of the spin response vector is reported in Fig. 2. It is seen that the qualitative behavior of R_x is similar to that of R_y. The only distinction is the different character of the spatial decay of the R_x and R_y components. Namely, while, at large z and t_0, R_y decays monotonously with minute oscillations, R_x has pronounced oscillations with higher amplitude. The latter property will

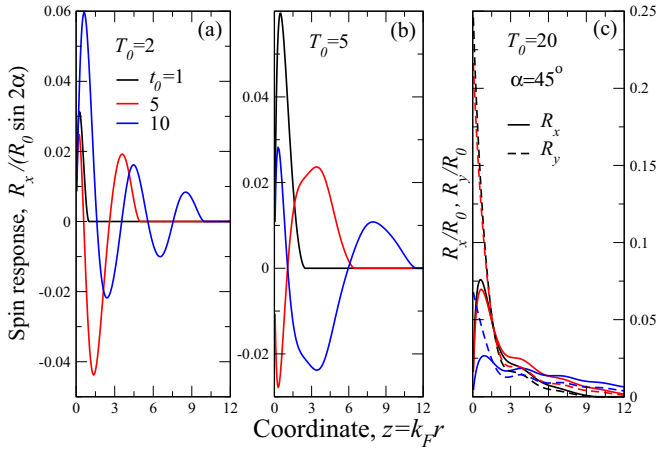

FIG. 2. The same as Fig. 1, but for the R_x component of the spin response vector. (a) (dimensionless spin-flip time $T_0 = 2$) and (b) ($T_0 = 5$) report the absolute value (i.e., that normalized by $\sin 2\alpha$) of the R_x component. Different dimensionless times t_0 are explained in the legend in (a). Panel (c) shows a comparison of the R_x (solid lines) and R_y (dashed lines) components for angle $\alpha = 45°$.

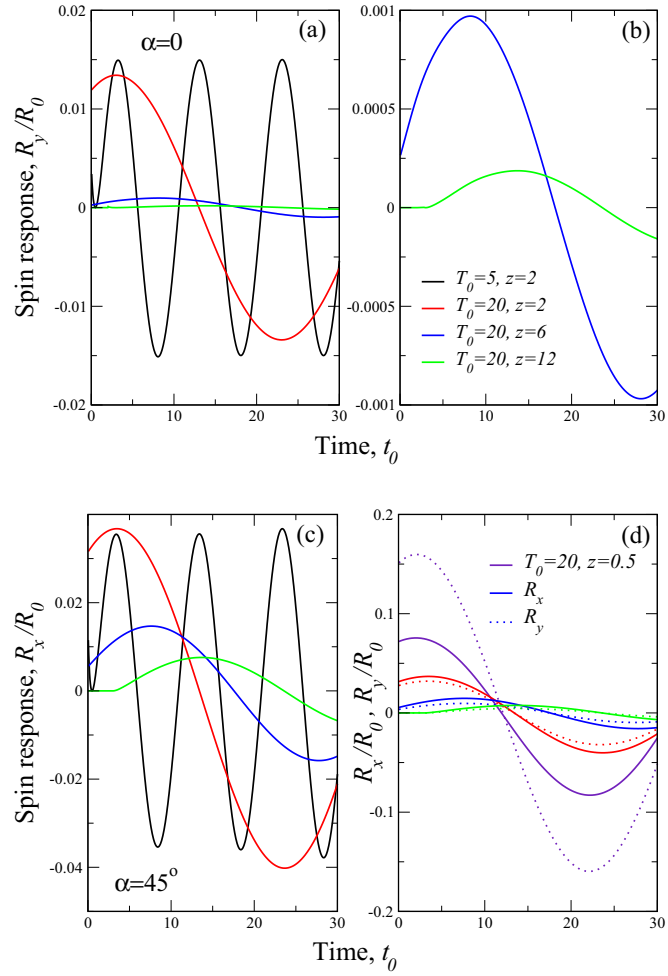

FIG. 3. Friedel oscillations of spin response components (a) and (b) R_y and (c) R_x as a function of dimensionless time t_0 for different spatial points z and spin-flip times T_0 as explained in (b) and (d). The curves in (b) are repeated from (a) on an expanded scale. (d) shows a comparison of the components R_x (solid lines) and R_y (dashed lines) as explained in the legend. (a) and (b) correspond to $\alpha = 0$, and (c) and (d) correspond to $\alpha = 45°$. All curves are plotted for $\tau_0 = 100$.

also be revealed in corresponding time dependences. On the other hand, a comparison of Figs. 1 and 2 shows that for the same angle α, R_y is always larger than R_x at small coordinates r. This becomes evident from Fig. 2(c), where a direct comparison of the components R_y and R_x is shown for $\alpha = 45°$ ($\sin 2\alpha = 1$) as at this angle the R_x component is largest. The reason is that at a small distance from the localized magnetic impurity the strongest response occurs for a component which is present without SOI twisting, i.e., R_y. This means that SOI influence occurs for substantially high distances from the localized spin. This is one more demonstration of the lag effect in spin response.

The temporal evolution of the spin response components R_x and R_y is reported in Fig. 3. The main result here is that, according to the corresponding spatial dependence in Fig. 1, the larger the dimensionless distance z to the impurity is, the smaller the amplitude of the Friedel oscillations is. This situation is shown in Figs. 3(a) and 3(c), where the amplitude of the corresponding oscillations is 3 [Fig. 3(c), $\alpha = 45°$] to 10 times [Fig. 3(a), $\alpha = 0$] smaller than that for $z = 2$. Moreover, as we saw in Fig. 2(c), at small distances from the magnetic impurity $z < 1$ the component R_y is larger than R_x. This situation is revealed in Fig. 3(d), where we compare the R_x and R_y components of the spin response vector. It is seen that at $z = 0.5$ the component $R_y > R_x$, while at higher $z = 2, 6, 12$, both components are almost equal to each other. This situation occurs for $\alpha = 45°$, where the R_x component is maximal. However, at other angles, the above qualitative regularity still occurs.

Figures 3(a) and 3(c) show also that the spin-flip time of the initial pulse T_0 determines the period of the Friedel oscillations of the spin response components. We can see from Figs. 3(a) and 3(c) that the half period of the Friedel oscillations is equal to approximately T_0: at $T_0 = 5$ it is approximately 5 [black curves in Figs. 3(a) and 3(c)], while at $T_0 = 20$ it is smaller than T_0, close to 15. Our analysis shows that at higher T_0, the oscillation period becomes progressively smaller than $2T_0$. This regularity also occurs in the entire admissible range of angles α. Apart from the diminishing amplitude of the oscillations at large z, there is one more important effect, namely, the time lag in the system response (corresponding, for instance, to the first maximum of Friedel oscillations of both the R_x and R_y components) as the distance from the magnetic impurity grows. Indeed, while at $z = 2$ the first maximum occurs at $t_0 \approx 2.5$, at higher distances the maximum (being much smaller than that at $z = 2$) occurs at $t_0 \approx 10$. This is detailed in Fig. 3(b), where we can see that while at $z = 6$ the first maximum occurs at $t_0 \approx 8$, at $z = 12$ it occurs at $t_0 \approx 15$. The same retardation effect is visible for the R_x component in Figs. 3(c) and 3(d) when the system response appears earlier at smaller distances from the impurity spin.

IV. DISCUSSION OF EXPERIMENTAL SITUATION AND OUTLOOK

Topological insulators and low-dimensional materials with spin-orbit interaction exhibit a large variety of interesting physical phenomena, which make them promising candidates for future spintronic applications [41]. We have shown here that the interplay of spin-orbit coupling and dynamic Friedel oscillations in the surface 2D electron gas in TIs reveals interesting effects like strong anisotropy of the system response to the rotation of a localized impurity spin. Specifically, the SOI-induced spin-momentum locking in TIs yields the anisotropic tensor structure of dynamic Friedel oscillations and generates a transient electric current, which is proportional to the dynamic spin. As both the dynamic spin response and SML-related transient current are due to the localized spin rotation (which acts for a finite time), the equilibrium versions of these quantities vanish. This fact is at odds with the case of an ordinary semiconductor (where SOI is absent) with massive electrons [37], where after a sufficiently long time, the dynamic Friedel oscillations yield an ordinary 2D RKKY interaction between localized spins [42].

Here, we calculated the spatial and temporal dependence of the dynamic spin response, which is proportional to the SML-related transient electric current. The need for such calculations may appear to explain theoretically some specific experimental situations. The presented model can describe adequately the propagation of spin excitation resulting from the fast optical or all-electrical reversal of a localized spin on the TI surface. Although our formalism captures the basic features of dynamic Friedel oscillations in TIs, the natural generalization should take into account a more general [than (1)] Hamiltonian which stems from a proper mapping of the exchange interaction between electrons and localized spins in the TI bulk to its surface states. Such a Hamiltonian was derived in Ref. [18], and it would be interesting to calculate the dynamic spin response and transient electric current within such a generalized approach.

One more generalization of our model is to consider the distortion of the initial Dirac cone, i.e., the unperturbed term (2) in the Hamiltonian (1). This distortion is usually thought of in the form of warping [43,44] and tilting [44,45]. Generally speaking, the warping of the initial Dirac cone emerges when one considers the expansion of the initial crystal lattice potential up to higher orders in wave vector $\mathbf{k}$ components. In the TI Bi_2Te_3, the warping of the initial Dirac cone has hexagonal symmetry due to that of the underlying crystal structure. These warping terms were introduced by Fu [43] in order to reproduce the angle-resolved photoemission spectroscopy experimental results, showing the deviation of the Fermi surface cross sections from the circular ones. In terms of the k_x and k_y components used here (rather than $k_\pm = k_x \pm ik_y$ used in the original paper [43]), this term reads $\Delta\mathcal{H} = \lambda\sigma_z k_x(k_x^2 - 3k_y^2)$, showing that it is significant only when we consider the out-of-plane properties of the TI. Moreover, as has been shown, these terms generate the additional (to those considered above) Friedel oscillations of the local density of states around *nonmagnetic*, i.e., *spinless,* defects (both point [43] and extended [46,47]) in STM experimental setups. The question of dynamic Friedel oscillations around magnetic impurity, to the best of our knowledge, has not been considered to date with respect to the above warping term. We note here that constant λ in the above warping term is very large at high charge carrier densities. As here we consider the small carrier density, the above warping corrections to the nonperturbed Hamiltonian (2) are small. However, it would be interesting to consider the contribution of the warping terms to the dynamic Friedel oscillations. This may be done along the lines of the present perturbative consideration as it may be possible to construct the unperturbed Green's function of the Hamiltonian with respect to warping terms.

Likewise, the Dirac cone tilting in the form $-t\sigma_x k_x$ (t is a tilt parameter) [44,45] can be included in the Hamiltonian (2). This term is remarkable as it breaks the time-reversal symmetry, which allows for backscattering of the (topologically protected in the initial Dirac cone) states and hence suppresses the spin-momentum locking. If the tilt is realized in TIs, it will alter the character of dynamic Friedel oscillations, making them less regular with a smaller amplitude compared to Figs. 2(a), 2(b), and 3. Also, the z component of the spin response, R_z, may appear. The magnitude of this effect depends on the tilting parameter value. From a technical point of view, this term may be well treated within the presented approach as it permits us to construct the unperturbed Green's function. Thus, theoretical studies of the joint action of the tilting and warping terms on the dynamical response of a TI electron gas would be interesting. We postpone these studies to future publications.

One more interesting physical problem directly related to the present consideration is the implications of the results obtained for the TI thin films. A key distinctive feature of a TI thin film compared to a slab of finite thickness is that in the former case there are two surfaces, say, top and bottom. Due to the small film thickness, the electronic states localized on the top and bottom surfaces are not independent. The coupling between the localized states on the two surfaces leads to additional effects absent in semi-infinite (sufficiently thick) slabs where only one surface is present. Static Friedel oscillations in thin films were considered in Ref. [48] for spin-independent Coulomb potentials. On the other hand, here, we consider magnetic impurities and the dynamical response to the impurity spin rotation. It was shown in [48] that at low charge carrier densities the TI thin films behave as ordinary conductors with parabolic carrier dispersion and like surfaces of the bulk TI at high densities. Our analysis of Figs. 1 and 2 shows that dynamic Friedel oscillations at large distances $z > 5$ decay as $\cos 2z/z^p$, where the exponent p depends on the spin-flip time duration T and angle α. Namely, for $\alpha = 45^\circ$ (Fig. 2) at dimensionless spin-flip time $T_0 = 2$, $p \approx 3.1$, while for $T_0 = 20$, $p \approx 4.8$. For $\alpha = 0$, which is the case for R_y (Fig. 1), the decay is faster, $p \approx 5.1$. This shows that although the logic of Ref. [48] applies also for our consideration, in the dynamic case we have more parameters, so the situation requires additional studies. The case of dynamic Friedel oscillations in TI thin films will be considered elsewhere.

The possible experimental methods for very fast reversal of spins localized on a TI surface can be found, for instance, in Refs. [30,39]. To access the controllable transient impurity spin dynamics, time-dependent driving of an adatom on the TI surface is needed while monitoring characteristics

like the magnetization of a neighboring adatom and time-dependent electric current leading to spin-momentum locking. For instance, the magnetic moment direction of a single $3d$ adsorbed adatom (Cr, Mn, Fe, and Co) can be controllably varied by changing the distance between the adatom and the STM tip [49]. Ultrafast temporal resolution can be enabled using pulsed electromagnetic fields acting on the localized spin moment of an adatom [50]. On the nanosecond timescale, spin-polarized STM experiments were realized [51] using voltage pulses to achieve the time resolution.

We note in this context that the spin-orbit interaction, being an integral part of the TI Hamiltonian, would facilitate spin reversal, so that TIs can be regarded as an almost ideal system for that. As we have shown, in addition to the tensor structure of the spin response, SOI also generates anisotropy in the TI plane, which is reflected in the appearance of the angle α. In this case, the picosecond spin flips in magnetic nanoparticles (possessing localized spins), reachable in TIs, may become shorter or longer depending on the SOI constant γ and anisotropy angle α. Note that SOI-induced anisotropy may interact with the natural anisotropy of a magnetic nanoparticle, thus limiting such spin rotation. This interesting effect will be considered elsewhere.

We finally mention the effects which may appear not only in TIs but also in other 2D systems (like semiconductor surfaces and interfaces), where Rashba SOI plays an important role. One such effect is related to the chaotic internal motion in 2D excitons due to SOI inclusion. The chaotic regime was studied in a recent paper [40] that showed such a chaotic regime may be important for photovoltaic devices fabricated from thin films of organometallic perovskites [52] and other 2D semiconductor structures. Chaotic behavior may also arise in the case studied here. Indeed, the irregular oscillatory behavior of the spin density, reported in Fig. 1, may be related to the possible onset of chaotic behavior. One can easily imagine a situation where some electron-hole interactions (like the Coulomb one in an exciton) in a 2D electron gas produce certain bound states, which may become unstable and thus prone to chaos. The manifestation of chaos is also present in the quantum case [53]. Another example is the ensemble of localized spins in a 2D semiconductor structure, which interact indirectly via the RKKY mechanism [41]. The most common case is that the impurity spins are distributed chaotically in a semiconducting host so that their separation is random. This may immediately lead to sub- or superdiffusive spin transport in these structures [39], which can be described by the introduction of fractional derivatives in the corresponding kinetic equations [54].

ACKNOWLEDGMENT

This work was supported by the National Science Center of Poland as Research Project No. DEC-2017/27/B/ST3/02881.

[1] C. Kittel, *Quantum Theory of Solids* (Wiley, New York, 1987).
[2] J. M. Ziman, *Principles of the Theory of Solids* (Cambridge University Press, Cambridge, 1979).
[3] M. Z. Hasan and C. L. Kane, Rev. Mod. Phys. **82**, 3045 (2010).
[4] D. Hsieh, Y. Xia, D. Qian, L. Wray, J. H. Dil, F. Meier, J. Osterwalder, L. Patthey, J. G. Checkelsky, N. P. Ong, A. V. Fedorov, H. Lin, A. Bansil, D. Grauer, Y. S. Hor, R. J. Cava, and M. Z. Hasan, Nature (London) **460**, 1101 (2009).
[5] S.-Y. Xu, Y. Xia, L. A. Wray, S. Jia, F. Meier, J. H. Dil, J. Osterwalder, B. Slomski, A. Bansil, H. Lin, R. J. Cava, and M. Z. Hasan, Science **332**, 560 (2011).
[6] D. Awschalom and N. Samarth, Physics **2**, 50 (2009).
[7] A. Dyrdał, J. Barnaś, and A. Fert, Phys. Rev. Lett. **124**, 046802 (2020); D. C. Vaz, F. Trier, A. Dyrdał, A. Johansson, K. Garcia, A. Barthélémy, I. Mertig, J. Barnaś, A. Fert, and M. Bibes, Phys. Rev. Materials **4**, 071001(R) (2020).
[8] B. A. Bernevig, T. L. Hughes, and S. C. Zhang, Science **314**, 1757 (2006).
[9] D. Hsieh, D. Qian, L. Wray, Y. Xia, Y. S. Hor, R. J. Cava, and M. Z. Hasan, Nature (London) **452**, 970 (2008).
[10] A. Manchon, H. C. Koo, J. Nitta, S. M. Frolov, and R. A. Duine, Nat. Mater. **14**, 871 (2015).
[11] E. Šimánek and B. Heinrich, Phys. Rev. B **67**, 144418 (2003).
[12] G. M. Genkin, Phys. Rev. B **55**, 5631 (1997).
[13] M. V. Costache, M. Sladkov, S. M. Watts, C. H. van der Wal, and B. J. van Wees, Phys. Rev. Lett. **97**, 216603 (2006).
[14] Q. Liu, C.-X. Liu, C. Xu, X.-L. Qi, and S.-C. Zhang, Phys. Rev. Lett. **102**, 156603 (2009).
[15] R. R. Biswas and A. V. Balatsky, Phys. Rev. B **81**, 233405 (2010).
[16] M. Schmid, W. Hebenstreit, P. Varga, and S. Crampin, Phys. Rev. Lett. **76**, 2298 (1996).
[17] M. F. Crommie, C. P. Lutz, and D. M. Eigler, Science **262**, 218 (1993).
[18] V. I. Litvinov, Phys. Rev. B **89**, 235316 (2014).
[19] J.-J. Zhu, D.-X. Yao, S.-C. Zhang, and K. Chang, Phys. Rev. Lett. **106**, 097201 (2011).
[20] D. A. Abanin and D. A. Pesin, Phys. Rev. Lett. **106**, 136802 (2011).
[21] T. Kampfrath, K. Tanaka, and K. A. Nelson, Nat. Photonics **7**, 680 (2013).
[22] L. L. Patera, F. Queck, P. Scheuerer, and J. Repp, Nature (London) **566**, 245 (2019).
[23] A. Kirilyuk, A. V. Kimel, and T. Rasing, Rev. Mod. Phys. **82**, 2731 (2010).
[24] T. Seifert *et al.*, Nat. Commun. **9**, 2899 (2018).
[25] E. M. Lifshitz and L. P. Pitaevskii, *Statistical Physics*, Part 2 (Pergamon Press, Oxford, 1980).
[26] J. Fransson, Phys. Rev. B **82**, 180411(R) (2010).
[27] S. R. Power, F. S. M. Guimaraes, A. T. Costa, R. B. Muniz, and M. S. Ferreira, Phys. Rev. B **85**, 195411 (2012).
[28] W. Chantrell, M. Wongsam, T. Schrefl, and J. Fidler, in *Encyclopedia of Materials: Science and Technology*, edited by K. H. J. Buschow, R. W. Cahn, M. C. Flemings, B. Ilschner, E. J. Kramer, and S. Mahajan (Elsevier, Amsterdam, 2001).
[29] S. Wienholdt, D. Hinzke, and U. Novak, Phys. Rev. Lett. **108**, 247207 (2012).

[30] G. Malinowski, F. Dalal Longa, J. H. H. Rietjens, P. V. Paluskar, R. Huijink, and H. J. M. Swagten, Nat. Phys. **4**, 855 (2008).
[31] S. Bhattacharjee, L. Nordström, and J. Fransson, Phys. Rev. Lett. **108**, 057204 (2012).
[32] M. R. Mahani, A. Pertsova, and C. M. Canali, Phys. Rev. B **90**, 245406 (2014).
[33] A. H. Castro Neto, F. Guinea, N. M. R. Peres, K. S. Novoselov, and A. K. Geim, Rev. Mod. Phys. **81**, 109 (2009).
[34] S. Das Sarma, S. Adam, E. H. Hwang, and E. Rossi, Rev. Mod. Phys. **83**, 407 (2011).
[35] V. K. Dugaev, V. I. Litvinov, and J. Barnaś, Phys. Rev. B **74**, 224438 (2006).
[36] H. Imamura, P. Bruno, and Y. Utsumi, Phys. Rev. B **69**, 121303(R) (2004).
[37] V. A. Stephanovich, V. K. Dugaev, V. I. Litvinov, and J. Berakdar, Phys. Rev. B **95**, 045307 (2017).
[38] *Handbook of Mathematical Functions*, edited by M. Abramowitz and I. I. Stegun, Applied Mathematics Series Vol. 55 (National Bureau of Standards, Washington, DC, 1964).
[39] M. Battiato, K. Carva, and P. M. Oppeneer, Phys. Rev. Lett. **105**, 027203 (2010).
[40] V. A. Stephanovich and E. Ya. Sherman, Phys. Chem. Chem. Phys. **20**, 7836 (2018).
[41] I. Žutić, J. Fabian, and S. Das Sarma, Rev. Mod. Phys. **76**, 323 (2004).
[42] V. I. Litvinov and V. K. Dugaev, Phys. Rev. B **58**, 3584 (1998).
[43] L. Fu, Phys. Rev. Lett. **103**, 266801 (2009).
[44] N. P. Armitage, E. J. Mele, and A. Vishwanath, Rev. Mod. Phys. **90**, 015001 (2018).
[45] T. O. Wehling, A. M. Black-Schaffer, and A. V. Balatsky, Adv. Phys. **63**, 1 (2014)
[46] Z. Alpichshev, J. G. Analytis, J.-H. Chu, I. R. Fisher, Y. L. Chen, Z. X. Shen, A. Fang, and A. Kapitulnik, Phys. Rev. Lett. **104**, 016401 (2010).
[47] T. Zhang, P. Cheng, Xi Chen, J.-F. Jia, X. Ma, K. He, L. Wang, H. Zhang, Xi Dai, Z. Fang, X. Xie, and Q.-K. Xue, Phys. Rev. Lett. **103**, 266803 (2009).
[48] W. E. Liu, H. Liu, and D. Culcer, Phys. Rev. B **89**, 195417 (2014).
[49] K. Tao, V. S. Stepanyuk, W. Hergert, I. Rungger, S. Sanvito, and P. Bruno, Phys. Rev. Lett. **103**, 057202 (2009).
[50] S. Eich, M. Plötzing, M. Rollinger, S. Emmerich, R. Adam, C. Chen, H. C. Kapteyn, M. M. Murnane, L. Plucinski, D. Steil, B. Stadtmüller, M. Cinchetti, M. Aeschlimann, C. M. Schneider, and S. Mathias, Sci. Adv. **3**, e1602094 (2017).
[51] S. Baumann, W. Paul, T. Choi, C. P. Lutz, A. Ardavan, and A. J. Heinrich, Science **350**, 417 (2015).
[52] S. D. Stranks and H. J. Snaith, Nat. Nanotechnol. **10**, 391 (2015).
[53] V. A. Stephanovich, E. Ya. Sherman, N. T. Zinner, and O. V. Marchukov, Phys. Rev. B **97**, 205407 (2018).
[54] P. Garbaczewski and V. A. Stephanovich, Phys. Rev. E **80**, 031113 (2009).